Supplementary Information

Geometry and Stability of Molecular Clusters: Factor to Be Considered in Biomolecular Activity

Noam G. da Silva,[a] Alexandre M. Alecrim,[b] Renyer A. Costa[a] and Kelson M. T. de Oliveira*[a]

[a]Laboratório de Química Teórica e Computacional, Departamento de Química, Universidade Federal do Amazonas, Campus Universitário, Setor Norte, Av. Rodrigo O. J. Ramos, 6200, Japiim, 69077-000 Manaus-AM, Brazil

[b]Instituto de Educação, Agricultura e Meio Ambiente, Universidade Federal do Amazonas, Campus Vale do Rio Madeira, R. 29 de Agosto, 786, Centro, 69800-000 Humaitá-AM, Brazil

Table S1 is an adaptation from published studies.[1] The results indicate that MelAc is inactive in comparison with Bet, BetAc and Lup. This inactivity gave rise to the problem studied in the present work.

Table S1. Half-maximal inhibitory concentration (IC_{50}) of antiplasmodial compounds isolated from plant species

Compound	IC_{50} against *P. falciparum*[a] / μM	
	3D7	Dd2
BetAc	5.60 ± 1.51	8.23 ± 0.69
MelAc	508.74 ± 5.02	710.10 ± 16.97
Lupeol	80.30 ± 2.15	54.22 ± 0.31
Betulin	17.08 ± 3.20	14.22 ± 0.03

[a]Published by Carmo *et al.*[1] IC_{50}: half-maximal inhibitory concentration; BetAc: betulinic acid; MelAc: melaleucic acid.

The total single point energies (E_T) were obtained for molecules optimized with AM1 (Table S2). The structure of both compounds is practically the same, suggesting that the energetic differences occur as a result of the difference in C27.

Table S2. Total single point energies (E_T) for 1M in gas phase, and with IEF-PCM implicit solvation, obtained by B3LYP/6-31+G(2d, p)//AM1 approach

Compound	E_T / (kJ mol^{-1})			ΔE^a / (kJ mol^{-1})	
	In gas phase	$CHCl_3$	$(CH_3)_2SO$	$CHCl_3$	$(CH_3)_2SO$
BetAc	–3,670,003.894	–3,670,025.145	–3,670,034.711	–21.251	–30.817
MelAc	–4,061,910.961	–4,061,938.687	–4,061,950.603	–27.726	–39.642

[a]E_T of molecule with IEF-PCM solvation minus E_T of molecule in gas phase. E_T: total single point energies; BetAc: betulinic acid; MelAc: melaleucic acid.

*e-mail: kelsonmota@ufam.edu.br

Specific theoretical vibrations of BetAc and MelAc are presented in Table S3. The presence of the additional carboxyl in MelAc causes the reduction of vibrational energy of C3O–H and C28OO–H. The more energetic stretchings of O1–H1, O2–H2 and C3–OH occur for BetAc. The stretching C29–H, C–H of the methyls and the rings, C20=C29, C28=O and C28–OH are more energetic for MelAc, which indicate a relaxation effect for these vibrations with the additional carboxyl, but this effect is neither observed for O–H nor for C3–OH bonds.

Table S3. Stretching (s) and bending (b) theoretical frequencies for 1M systems of BetAc and MelAc, obtained by B3LYP/6-31G(d) approach in gas phase

Bond involved (vibration type)	Frequency / cm^{-1}		
	BetAc	MelAc	Experimental[a]
O1–H1 (s)	3831.50	3830.42	3438
O2–H2 (s)	3742.83	3741.74	3438
O4–H4 (s)	–	3737.64	3438
C29–H (s)	3130.58-3067.74	3130.93-3068.32	2943
C–H (methyl and rings) (s)	2948.99-268 8.56	2958.19-2685.79	2870
C20=C29 (s)	1738.94	1739.88	1693
C27=O (s)	–	1696.83	1642
C28=O (s)	1712.86	1713.38	1642
C3–OH (s)	1110.85	1107.37	1038[b]
C27–OH (s)	–	1132.57	1038[b]
C28–OH (s)	1124.84	1127.44	1038[b]
C–H (methyl and rings) (b)	1595.97-1433.86	1592.69-1434.59	1451
C29–H (b)	1365.78-1310.75	1364.58-1312.27	1320
C–C (rings) (b)	994.42-20.68	998.50-23.95	792

[a]Published by Pînzaru *et al.*;[2] [b]published by Pai *et al.*[3] BetAc: betulinic acid; MelAc: melaleucic acid; s: stretching; b: bending.

The physical properties listed in Table S4 show that the additional carboxyl of MelAc causes increased interaction between the molecules. All properties are higher for MelAc, indicating consistency in the effect of carboxyl.

Table S4. Main physical properties of the compounds

Property	BetAc	MelAc
Melting point / °C (at 760 mm Hg)	295-298[a]	363-364[b]
Boiling point[c] / °C (at 760 mm Hg)	550.020	615.420
Enthalpy of vaporization[c] / (kJ mol^{-1})	95.407	104.692
Density[c] / (g cm^{-3})	1.065	1.200
Surface tension[c] / (dyne cm^{-1})	39.983	46.657

[a]Obtained with Matrix Scientific Catalog;[4] [b]published by Chopra *et al.*[5] and Arthur *et al.*;[6] [c]obtained with ACD/Labs Percepta Platform.[7] BetAc: betulinic acid; MelAc: melaleucic acid.

The geometric properties in Figures S1 and S2 show that the approaches result in data close to experimental. In addition, it is found that AM1 provides optimization data close to B3LYP, which supports the use of mixed approaches.

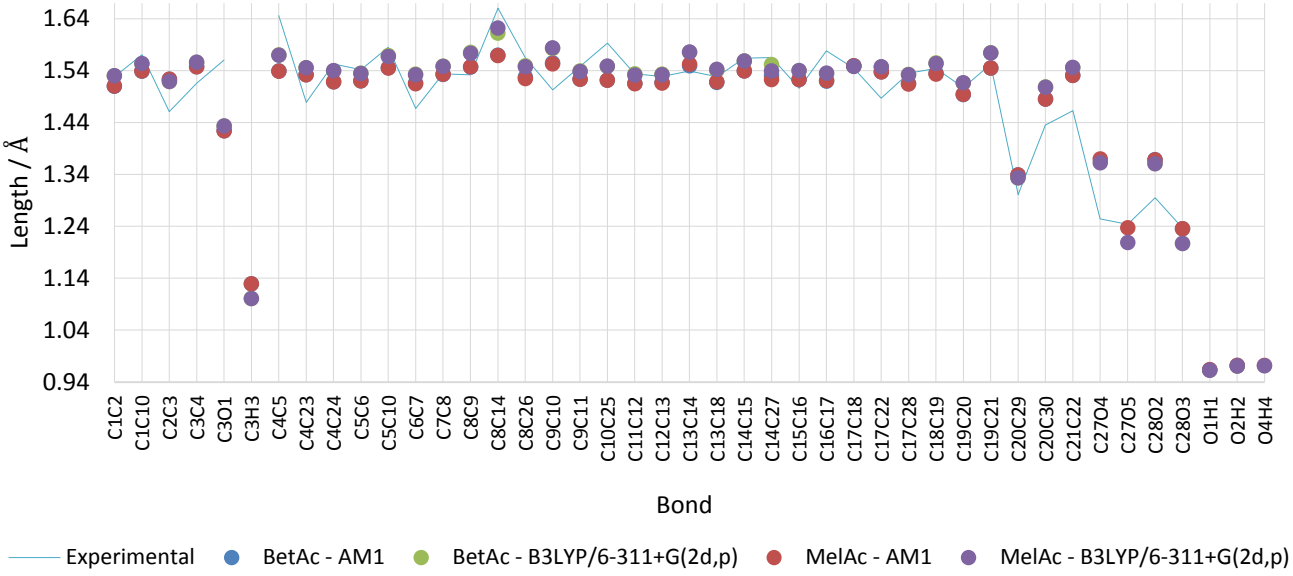

Figure S1. Lengths of interatomic bindings of both compounds after different optimization approaches, compared to methyl melaleucate iodoacetate experimental data.[8]

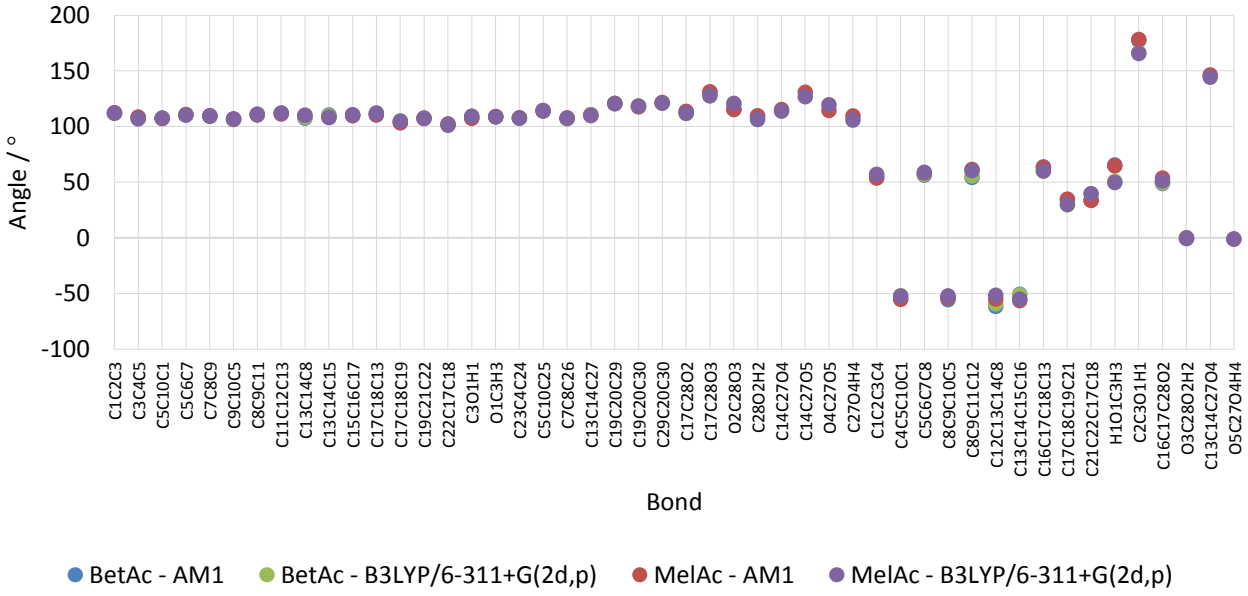

Figure S2. Interatomic angles of both compounds after different optimization approaches, indicating their similarity.

The IR spectra are extremely similar for BetAc and MelAc (Figure S3), and are close to the experimental.[2] At 3100 cm^{-1} region, both compounds exhibit two peaks, but only one peak is observed experimentally. These differences may occur due to differences in theoretical and experimental conditions.

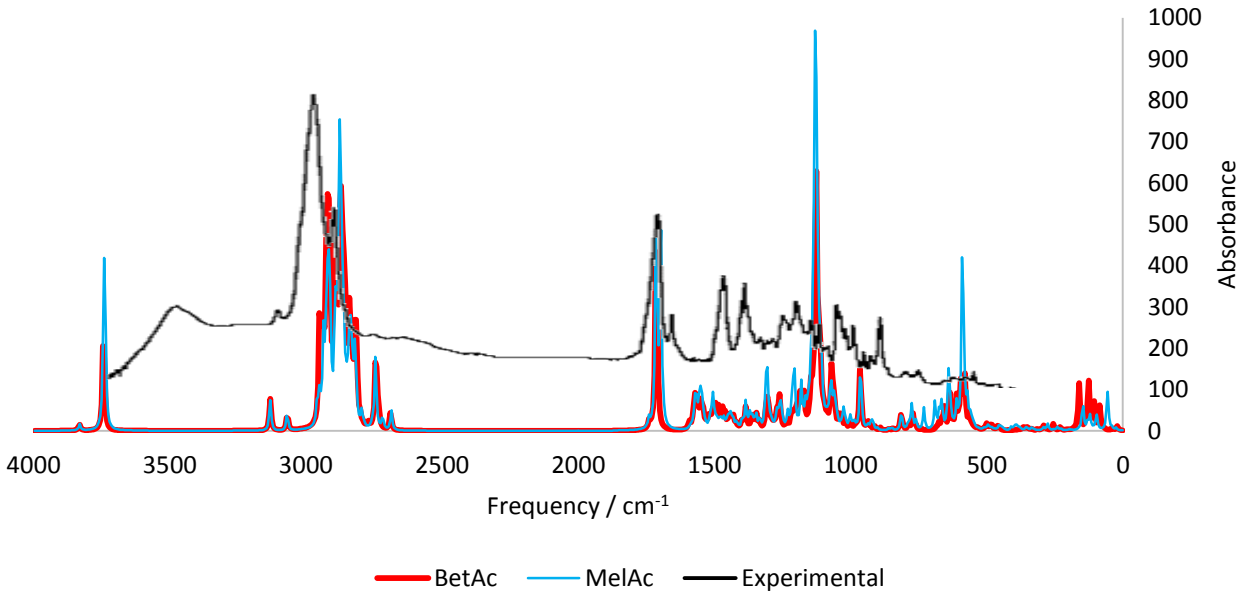

Figure S3. Experimental IR spectra for BetAc (black line) and theoretical IR spectra for BetAc and MelAc, obtained by B3LYP/6-31G(d) approach in gas phase.[2]

The Raman theoretical spectra of BetAc and MelAc are presented in Figure S4. The largest difference occurs in the 3050 cm^{-1} region, where both compounds exhibit two peaks, but only one peak is observed experimentally. The theoretical spectra exhibit two well-defined peaks in this region corresponding to the C29–H bond, with two distinct vibrations: synchronized stretching (3067.74 cm^{-1}) and alternating stretching (3130.58 cm^{-1}). The experimental signal, which is influenced by the conditions of the crystalline structure, occurs at 2944 cm^{-1} as a single band.

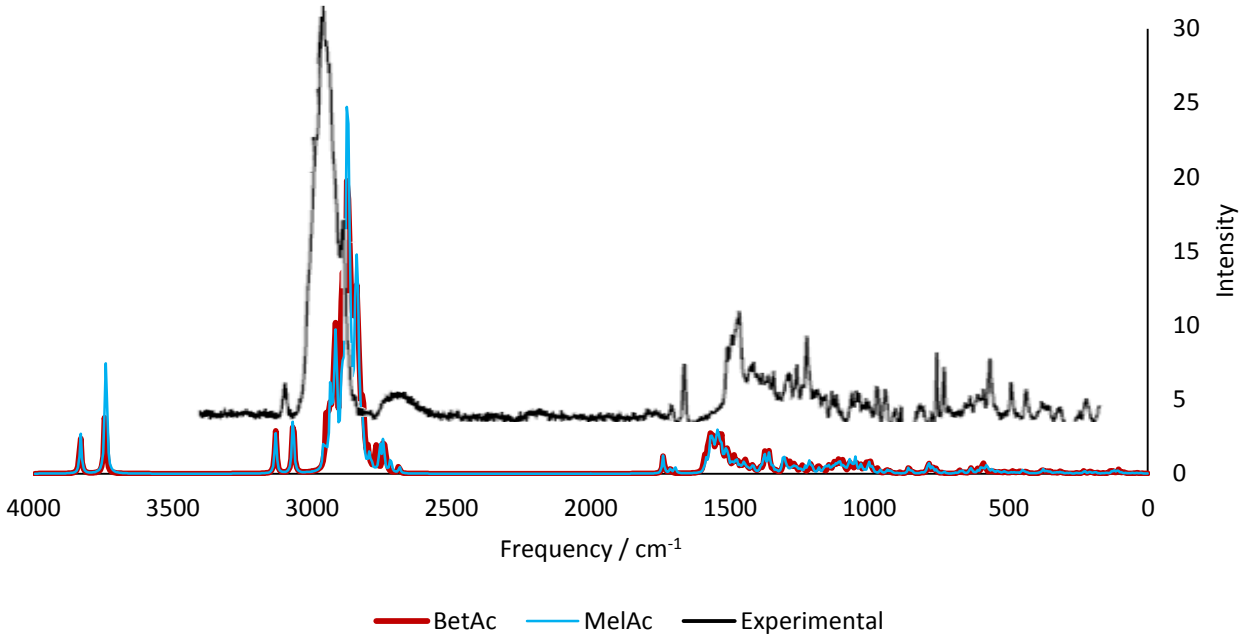

Figure S4. Experimental Raman spectra obtained for BetAc and theoretical spectra for both compounds, obtained by B3LYP/6-31G(d) approach in gas phase.[9]

Theoretical ^{13}C NMR data of BetAc and MelAc are presented in Figure S5. The highest difference occurs in C14 due to the additional carboxyl, having a stronger coupling, and in C27 relative to the carboxyl itself. All other signals are very close in both compounds, indicating that the electronic structures are similar, and that the additional carboxyl on MelAc has a limited local impact.

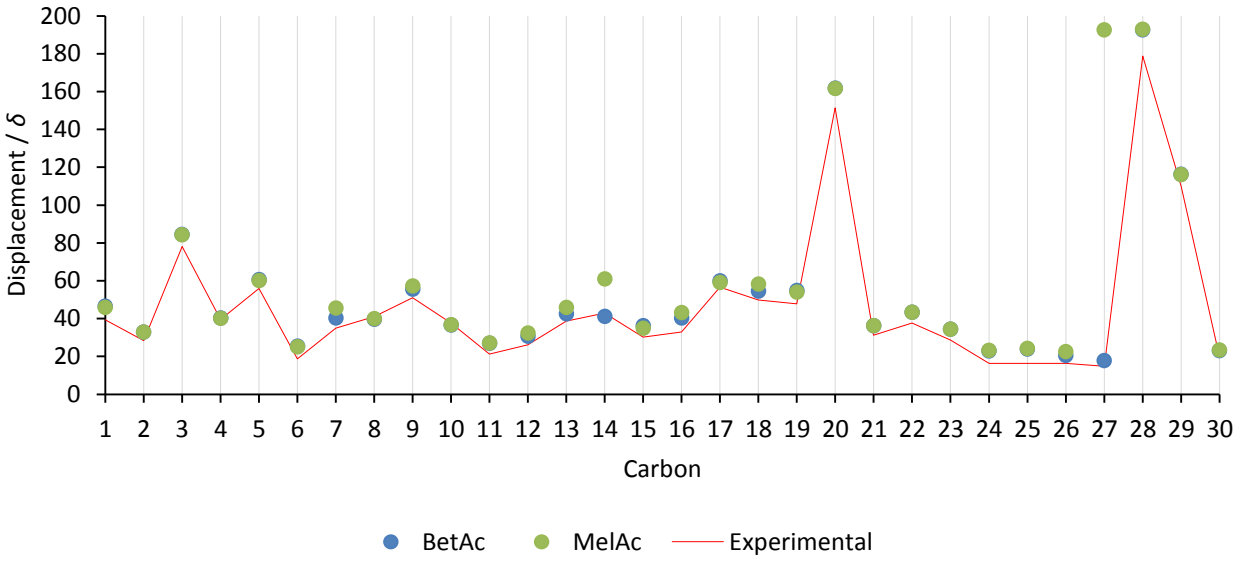

Figure S5. Comparison between experimental values of ^{13}C NMR of BetAc and theoretical values of both compounds, obtained by B3LYP/6-311++G(2d,p)//AM1 $CHCl_3$/IEF-PCM approach.[10]

The geometries of 2M systems are presented in Figure S6. Even with the possibility of formation of hydrogen bonds between the carboxyl at the C17 position and the hydroxyl at the C3 position, BetAc forms an even more unstable dimer than MelAc. The geometry of the 3M allows a more effective approximation of the polar groups at C17 and C3 (Figure S7). The hydrogen bonds occur with greater intensity, and the system is more stable in comparison with 1M and 2M.

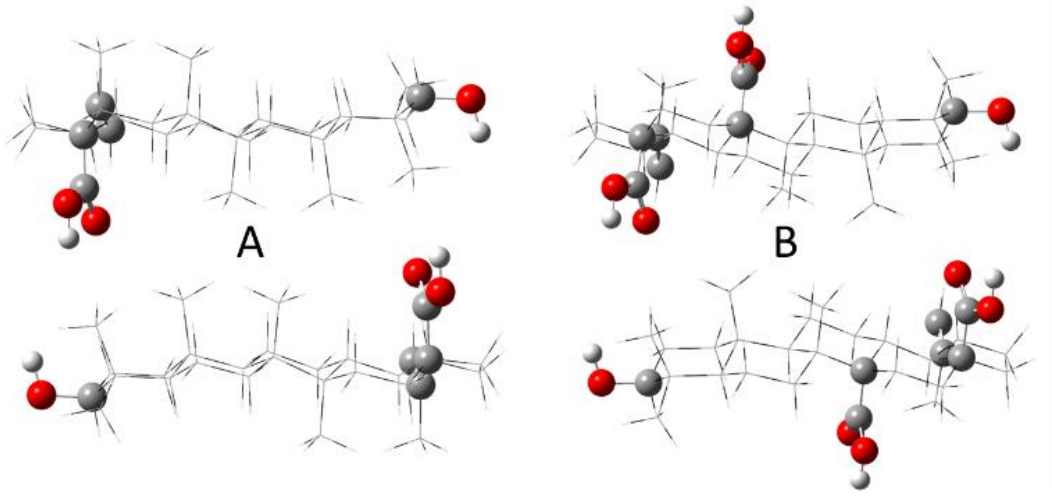

Figure S6. (A) BetAc and (B) MelAc 2M systems after AM1 optimization, highlighting the carboxyl and hydroxyl groups.

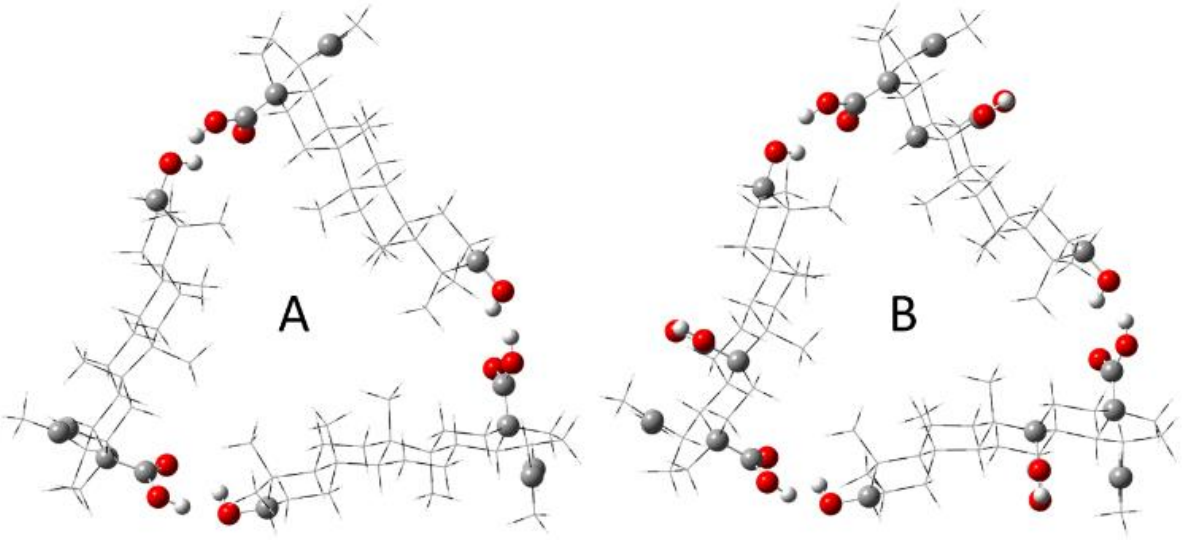

Figure S7. (A) BetAc and (B) MelAc 3M systems after AM1 optimization, highlighting the carboxyl and hydroxyl groups.

Five comparison compounds were used in the studies involving log P (Figure S8). With the comparisons we could observe that even with different log P values, the four LPT should have comparable activities. Messagenic acid A, derived from BetAc, was also analyzed in terms of MEPS (Figure S9). The results indicate that MelAc would not be inactive just because it had a polar group at C14. Compared to MelAc, messagenic acid A has a more polar distribution at the C14 region, and exhibits even better activity than BetAc.

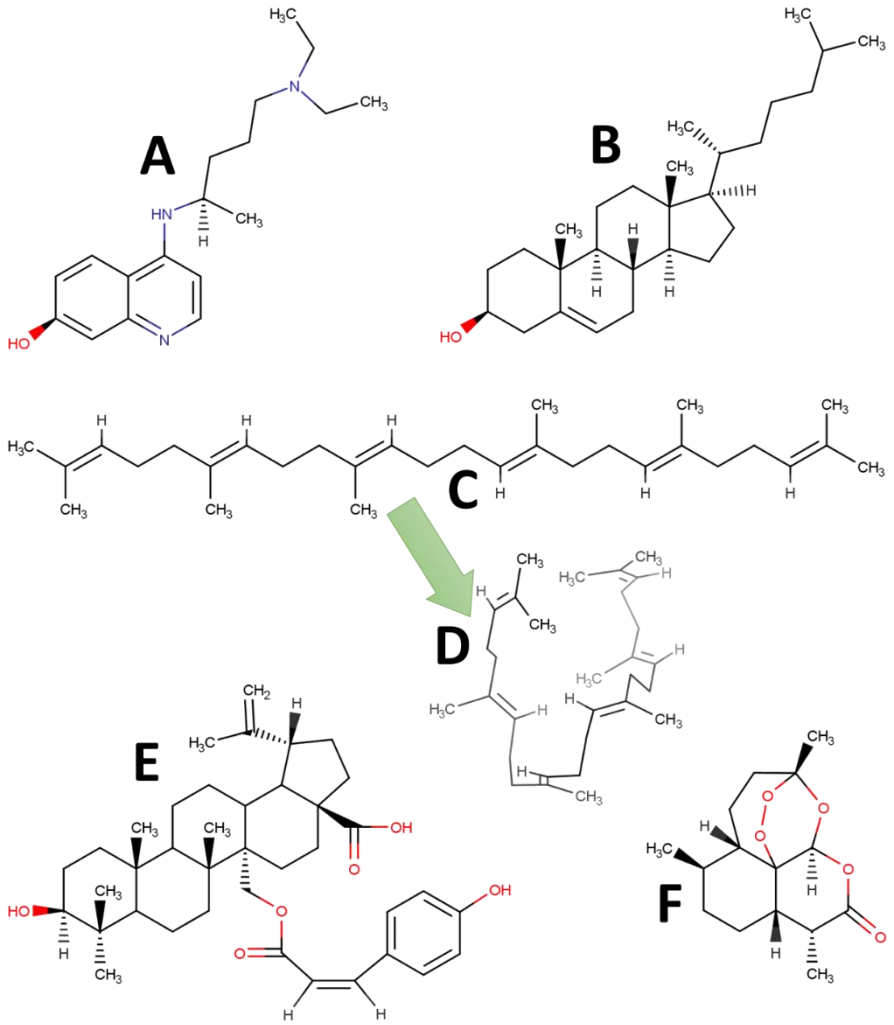

Figure S8. Structures of (A) *R*-chloroquine; (B) cholesterol; squalene in (C) linear and (D) curved form; (E) messagenic acid A; and (F) artemisinin.

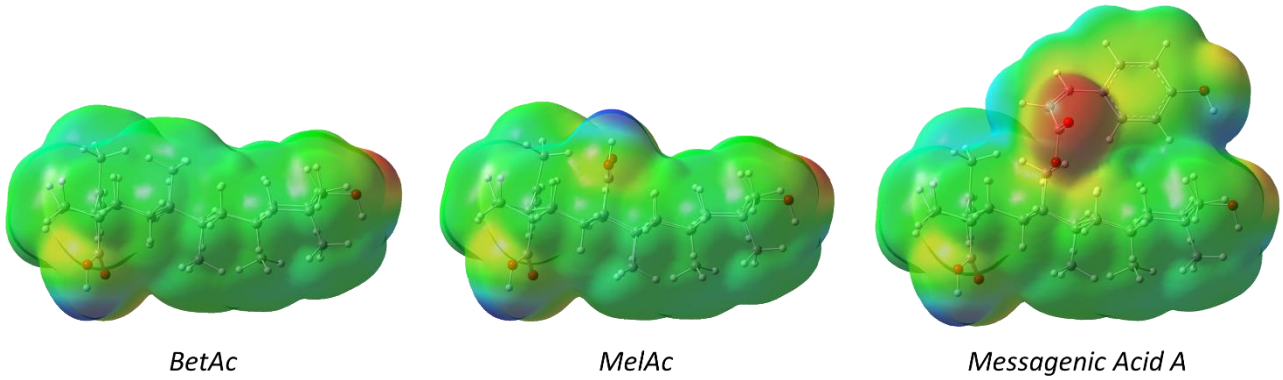

Figure S9. MEPS comparisons between the C27 regions of BetAc, MelAc, and messagenic acid A, obtained by B3LYP/6-311G//AM1 approach in gas phase.

In HSA docking (Figure S10), it is verified that M1 ↔ M1 overlaps occur with high molecular coincidence in all sites, suggesting great proximity of both compounds when interacting with this protein. As result, both compounds should be carried through the body.

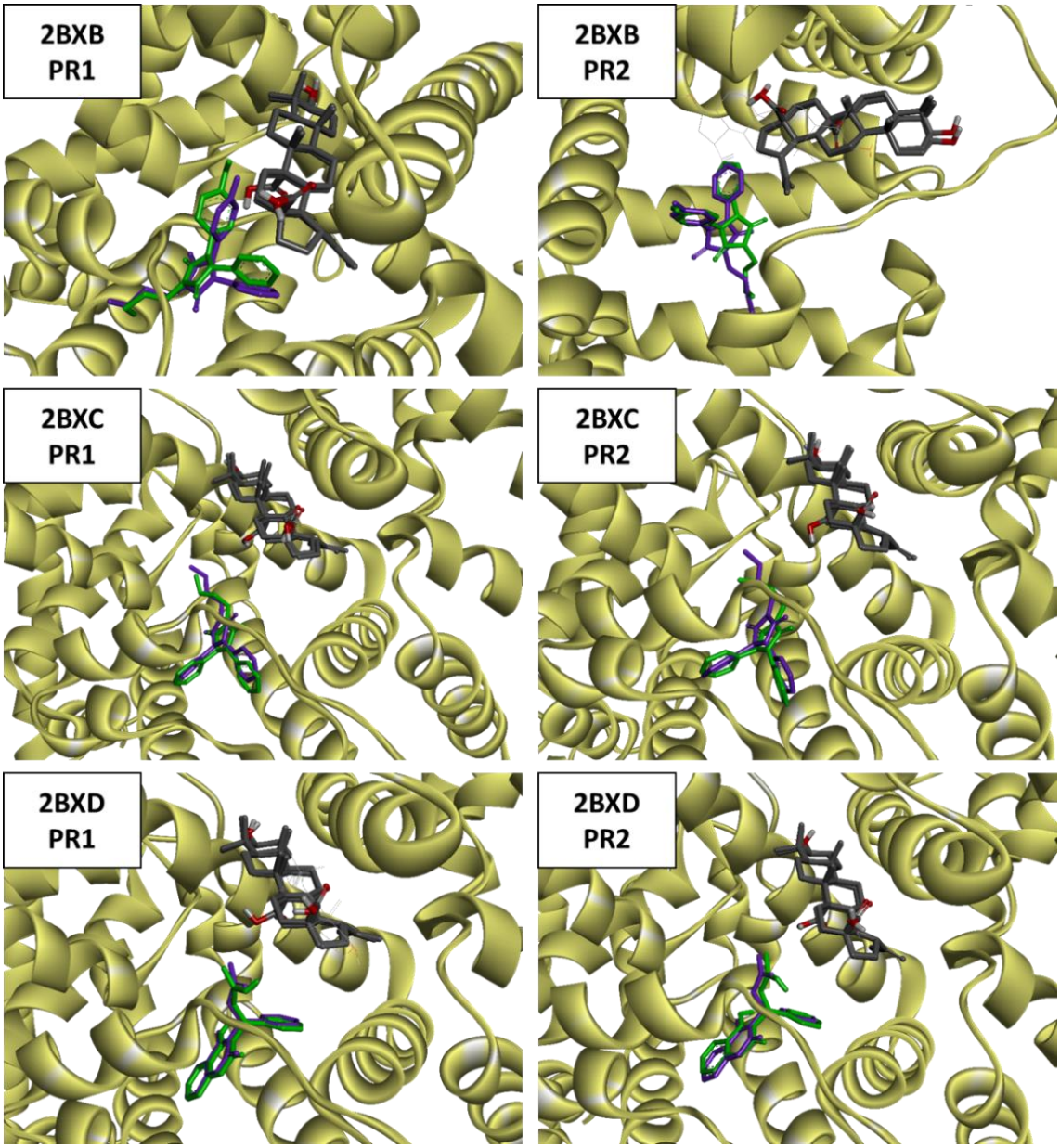

Figure S10. Redocked OL in HSA (2BXB, 2BXC, and 2BXD), with best affinity (in green) compared with non-redocked OL (in purple).

The modes for 1CET indicate that MelAc should have comparable activity to the other three LPT considered (Figure S11). This protein is complexed with chloroquine, a reference in terms of antimalarial activity. MelAc presents similar affinities to OL (chloroquine) and to the other NL, and additionally, this compound binds at same regions. Neither affinities nor docking modes indicate distinct behavior for MelAc, and the M1 ↔ M1 overlap on this protein occurs with good molecular coincidence. 5LSG corresponds to a protein complexed with BetAc, and redocking provided only one coupling mode, with optimal affinity and RMSD (also in Figure S11). Bet and Lup have great M1 ↔ M1 overlap with BetAc, and it is impossible to see them in the Figure. At this site, the good overlap also indicates comparable behaviors of compounds.

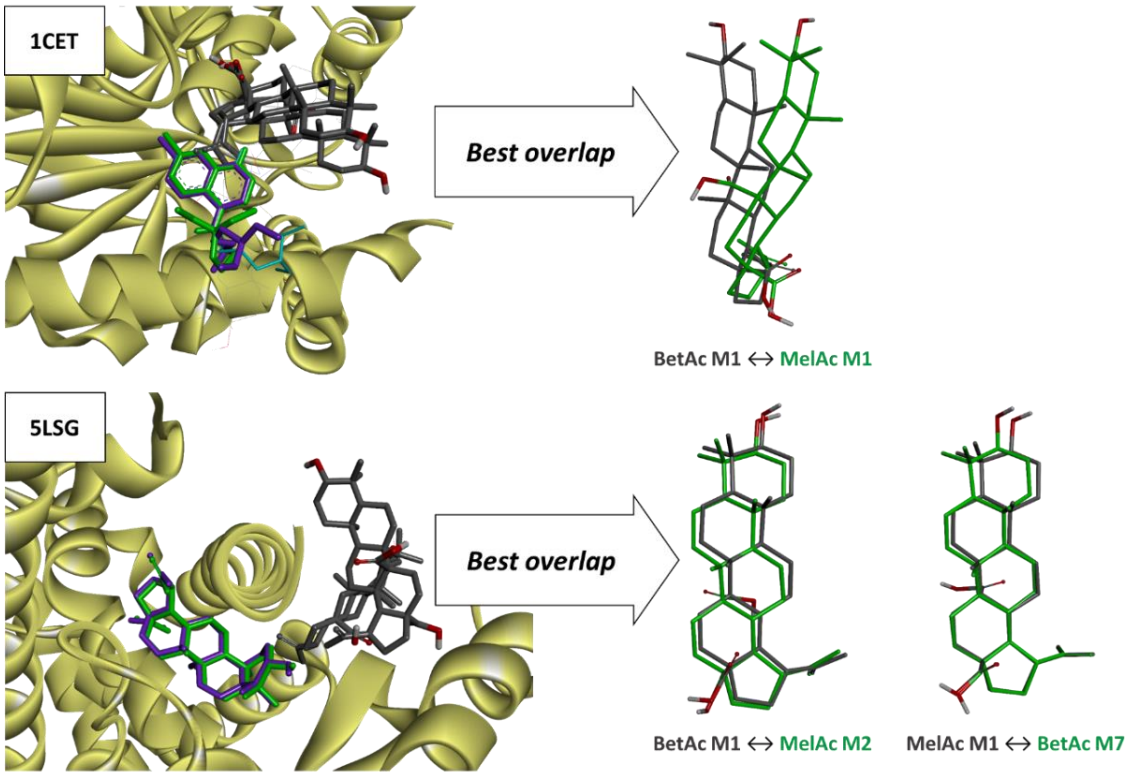

Figure S11. Redocked OL in 1CET and 5LSG, with best affinity (in green) and best RMSD (in blue) compared with non-redocked OL (in purple), and sites where compounds show better affinities, highlighting best overlaps (grey C-skeleton for higher affinity modes and green C-skeleton for closer overlap).

References

1. Carmo, D. F. M.; Amaral, A. C. F.; Machado, M.; Lopes, D.; Echevarria, A.; Rosário, V. E.; Silva, J. R. A.; *Pharmacogn. Mag.* **2015**, *11*, 244.
2. Pînzaru, S. C.; Leopold, N.; Kiefer, W.; *Talanta* **2002**, *57*, 625.
3. Pai, S. R.; Nimbalkar, M. S.; Pawar, N. V.; Dixit, G. B.; *Ind. Crops Prod.* **2011**, *34*, 1458.
4. http://www.matrixscientific.com/, accessed in May 2018.
5. Chopra, C. S.; Cole, A. R. H.; Theiberg, K. J. L.; White, D. E.; Arthur, H. R.; *Tetrahedron* **1965**, *21*, 1529.
6. Arthur, H. R.; Cole, A. R. H.; Thieberg, K. J. L.; White, D.; *Chem. Ind.* **1956**, *35*, 926.
7. ACD/Labs; *ACD/Labs Percepta Platform, Version 15.01*; Advanced Chemistry Development Inc., Toronto, ON, Canada, 2015.
8. Hall, S. R.; Maslen, E. N.; *Acta Crystallogr.* **1965**, *18*, 265.
9. Fălămaş, A.; Pînzaru, S. C.; Dehelean, C. A.; Peev, C. I.; Soica, C.; *J. Raman Spectrosc.* **2011**, *42*, 97.
10. Cichewicz, R. H.; Kouzi, S. A.; *Med. Res. Rev.* **2004**, *24*, 90.